JOURNAL OF SOLID STATE CHEMISTRY **95**, 352–359 (1991)

# Hydrothermal Synthesis, Structure, and Magnetic Properties of a New Polymorph of Lithium Vanadyl(IV) Orthophosphate: β-$LiVOPO_4$

K. H. LII AND C. H. LI

*Institute of Chemistry Academia Sinica, Nankang, Taipei, Taiwan, Republic of China*

AND C. Y. CHENG AND S. L. WANG

*Department of Chemistry, National Tsing Hua University, Hsinchu, Taiwan, Republic of China*

Received January 28, 1991; in revised form July 5, 1991

A new polymorph of lithium vanadyl(IV) orthophosphate, β-$LiVOPO_4$, has been synthesized hydrothermally in a sealed quartz glass tube under autogeneous pressure by slowly cooling from 450°C a mixture of $Li_2O$, $VO_2$, and 7.25 *M* $H_3PO_4$. This metastable compound has been characterized through a combination of techniques including single-crystal X-ray diffraction, differential thermal analysis, electron paramagnetic resonance, and magnetic susceptibility measurements. It crystallizes in the orthorhombic space group *Pnma* with $a = 7.444(2)$, $b = 6.300(1)$, $c = 7.174(2)$ Å, $V = 336.4(2)$ Å$^3$, $Z = 4$, and $R = 0.0248$. Its framework consists of infinite chains of corner-shared $VO_6$ octahedra, parallel to the *a*-axis, cross-linked by corner-shared $PO_4$ tetrahedra. These infinite chains have alternating short and long V–O bonds and are similar to those found in β-$VOPO_4$. The Li atom has six close oxygen neighbors. The $\beta \rightarrow \alpha$-$LiVOPO_4$ phase transition is reconstructive and occurs at ~750°C. The magnetic susceptibility is analyzed considering the expression of Bonner and Fisher for $S = 1/2$ ions isotropically coupled in antiferromagnetic linear chains. © 1991 Academic Press, Inc.

## Introduction

We have recently synthesized and structurally characterized a large number of new structures in the vanadium phosphate system using high-temperature solid state reactions and hydrothermal methods. Compounds such as $Cs_2V_3P_4O_{17}$ (*1*), β-$K_2V_3P_4O_{17}$ (*2*), $A_2VOP_2O_7$ ($A$ = Cs, Rb) (*3*), $AVP_2O_7$ ($A$ = Li–Cs) (*4–6*), $RbV_3P_4O_{17+x}$ (*7*), $KV_3P_4O_{16}$ (*8*), and $Zn_2VO(PO_4)_2$ (*9*) were prepared by solid state reactions. In hydrothermal experiments, we have found $K_2(VO)_3(HPO_4)_4$ (*10*), $K_2(VO)_2P_3O_9(OH)_3 \cdot 1.125H_2O$ (*11*), $A_{0.5}VOPO_4 \cdot xH_2O$ ($A$ = Na, $x$ = 2.0; $A$ = K, $x$ = 1.5) (*12*), and $Ni_{0.5}VOPO_4 \cdot 1.5H_2O$ (*13*). The hydrothermal method, in contrast to the solid state synthesis, is particularly well suited to the synthesis of low-temperature phases and metastable compounds. In order to discover new phases, we have used hydrothermal methods for the synthesis of compounds that had been prepared by high-temperature solid state reactions.

Among the $AVOPO_4$ ($A$ = Li, Na, K) phases, $KVOPO_4$ was prepared by the hydrothermal method (*14*), $LiVOPO_4$ by high-

0022-4596/91 $3.00

temperature solid state reaction (*15*), and $NaVOPO_4$ by either method (*16*). The compound $KVOPO_4$ is particularly interesting, since it is isostructural with the well-known nonlinear optical material $KTiOPO_4$. We have now found that crystals of a new polymorph of $LiVOPO_4$ can be grown under hydrothermal conditions. In this report, we describe the hydrothermal synthesis, single-crystal X-ray structure, thermal analysis, EPR, and magnetic susceptibility of β-$LiVOPO_4$, and compare its structure with the α-polymorph previously prepared by the solid state method.

## Experimental

### *Synthesis*

$Li_2O$ (99.9%) and $VO_2$ (99.5%), which were obtained from Cerac Inc., were used as received. $H_3PO_4$ (85%) was obtained from Merck. The i.d. of the quartz glass tube was 0.8 cm and the o.d. was 1.0 cm. The experiment was based on the method of Rabenau for the hydrothermal synthesis of chalcogenides (*17*). Typical reactions consisted of sealing 0.0886 g $Li_2O$, 0.4912 g $VO_2$, and 2.7 ml of 7.25 *M* $H_3PO_{4(aq)}$ solution in a quartz glass tube 10 cm in length (molar ratio Li : V : P = 1 : 1 : 3.3). The degree of fill was found to be 55% including the volume of undissolved $VO_2$. The glass ampoule was inserted into a cold-seal pressure vessel (TemPres MRA 112R), and the free volume remaining in the bore hole was determined using water measured from a buret. The water was subsequently removed from the bore hole. To counterbalance the pressure inside the ampoule, water was used. In order to prevent an explosion, the degree of fill in the cold-seal vessel outside the quartz glass tube was 60%. The closed end of the pressure vessel was inserted into a tube furnace, while the joint remained on the outside. The pressure vessel was maintained at 450°C and autogeneous pressure for 2 days and then cooled to room temperature at ca. 30°C/hr.

TABLE I

X-RAY POWDER DIFFRACTION DATA FOR β-$LiVOPO_4$[a]

| *hkl* | $d_{calcd}$ (Å) | $d_{obsd}$ (Å) | $2\theta_{obsd}$ (°) | $I_{obsd}$ |
|---|---|---|---|---|
| 101 | 5.166 | 5.163 | 17.16 | 15.8 |
| 011 | 4.733 | 4.736 | 18.72 | 28.9 |
| 111 | 3.994 | 3.994 | 22.24 | 7.9 |
| 200 | 3.722 | 3.720 | 23.90 | 5.2 |
| 002 | 3.587 | 3.590 | 24.78 | 28.9 |
| 201 | 3.304 | 3.305 | 26.95 | 100.0 |
| 102 | 3.231 | 3.231 | 27.58 | 31.6 |
| 020 | 3.150 | 3.145 | 28.29 | 68.4 |
| 211 | 2.926 | 2.928 | 30.50 | 13.0 |
| 112 | 2.875 | 2.875 | 31.08 | 13.0 |
| 121 | 2.689 | 2.687 | 33.32 | 11.8 |
| 202 | 2.583 | 2.584 | 34.69 | 7.9 |
| 220 | 2.404 | 2.410 | 37.28 | 5.2 |
| 221 | 2.280 | 2.278 | 39.52 | 3.4 |
| 122 | 2.256 | 2.256 | 39.92 | 17.1 |
| 013 | 2.236 | 2.236 | 40.30 | 10.5 |
| 113 | 2.141 | 2.142 | 42.16 | 6.0 |
| 302 | 2.041 | 2.041 | 44.35 | 2.5 |
| 031 | 2.015 | 2.012 | 45.01 | 15.8 |
| 400 | 1.861 | 1.861 | 48.89 | 5.2 |
| 230 | 1.829 | 1.826 | 49.90 | 2.5 |

[a] Orthorhombic; $a = 7.446(3)$, $b = 6.292(2)$, and $c = 7.177(3)$ Å; $\lambda = 1.5405$ Å.

The cooled glass ampoule was rolled in several layers of paper and opened by tapping with a hammer. The resulting green crystalline solid was removed, washed with water, rinsed with ethanol, and dried in a desiccator at ambient temperature. Visual microscopic inspection showed that the product contained many green crystals. Powder X-ray diffraction analysis indicated a single-phase β-$LiVOPO_4$ had been produced. The indexed pattern of β-$LiVOPO_4$ recorded at room temperature by using a Rigaku powder diffractometer with filtered copper radiation is given in Table I. The contents of Li, V, and P of a single-phase product were analyzed by using an ICP-AE spectrometer after dissolving the sample in 8 *N* $HNO_3$. Anal. Calcd for $LiVOPO_4$: Li, 4.11%; V, 30.17%, P, 18.34%. Found: Li, 4.27%; V, 30.8%; P, 18.6%. The compound appeared somewhat hygroscopic in the laboratory atmosphere. β-$LiVOPO_4$ was also obtained as a major product by heating a reaction mixture of $VO_2$ (2.00 g), $Li_2O$ (0.360 g), and 10 ml of 7.25 *M* $H_3PO_4$ in a 23-ml Teflon-lined stainless steel autoclave at 230°C for 4 days and then furnace-cooled to ambient temperature in about 10 hr. The sample prepared at 450°C was used for thermal analysis, magnetic susceptibility, and EPR measurements.

It was found that β-$LiVOPO_4$ could only be prepared hydrothermally. Solid state reactions of a mixture of $Li_2O$, $VO_2$, and $P_2O_5$ in a 1 : 2 : 1 molar ratio in sealed silica tubes at 650–750°C yielded α-$LiVOPO_4$ only. The solid state reaction did not occur at an appreciable rate below ~600°C. By taking the β-polymorph prepared hydrothermally and subsequently heating it at 750°C for 12 hr and then furnace-cooling to r.t., it was then found to transform to the α-polymorph. The α-polymorph, once formed, did not convert to the β-polymorph.

### *Thermal Analysis*

Differential thermal analysis (DTA) was performed on β-$LiVOPO_4$, using a DuPont DTA system. The experiments were performed in a $N_2$ atmosphere with both the heating and cooling rates at 8°C/min in the temperature range from r.t. to 850°C. Alumina was used as the reference. The sample gave an endothermic peak at ~780°C on heating. The peak was preceded by a premonitory drift in the baseline and the onset temperature was ~750°C. On cooling the sample did not show either an exothermic or an endothermic peak.

### *Single-Crystal X-ray Diffraction*

A green crystal having the dimensions 0.40 × 0.12 × 0.10 mm was selected for indexing and intensity data collection on a Nicolet R3m/V diffractometer with graphite-monochromated Mo$K\alpha$ radiation. The crystal was protected from the atmosphere with a layer of epoxy cement. Axial oscillation photographs along the three axes were taken to check the symmetry properties and unit cell parameters. Of the 331 unique reflections measured (maximum $2\theta = 50°$, octants collected $+h$, $+k$, $+l$, scan mode $\omega - 2\theta$), 307 reflections were considered observed ($I > 2.5\sigma(I)$) after Lp and empirical absorption corrections. Corrections for absorption were based on $\psi$ scans of a few suitable reflections with $\chi$ values close to 90° (*18*). Based on intensity statistics, extinction conditions, and successful solution and refinement of the structure, the space group was determined to be *Pnma* (No. 62). The structure was solved by direct methods and successive Fourier synthesis, and refined by full-matrix least-squares refinement based on *F* values. All of the atoms were refined with anisotropic temperature factors. All calculations were performed on a DEC MicroVAX II computer system using SHELTXL-Plus programs (*19*). Neutral-atom scattering factors and corrections for anomalous dispersion were from common sources (*20*). The multiplicity of the Li atom was allowed to refine but did not deviate significantly from full occupancy. Therefore, the Li site was considered fully occupied in subsequent refinement. The final cycle of full-matrix least-squares refinement gave $R$ and $R_w$ values of 0.0248 and 0.0278, respectively. The final difference map was flat to less than ±0.54 e/Å$^3$.

### *Magnetic Measurements*

A 72.8-mg powder sample was used to collect variable-temperature magnetic susceptibility $\chi(T)$ data from 4 to 300 K in a magnetic field of 3 kG using a Quantum Design SQUID magnetometer. As suggested by Selwood (*21*), diamagnetic contributions for $Li^+$, $V^{4+}$, $P^{5+}$, and $O^{2-}$ were estimated, which were subtracted from the experimental susceptibility data to obtain the molar

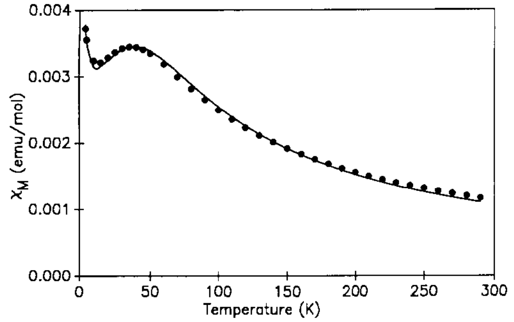

FIG. 1. Molar magnetic susceptibility ($\chi_M$) vs $T$ for polycrystalline $\beta$-LiVOPO$_4$. The smooth curve represents a fit to the Bonner and Fisher linear-chain model, Eq. (1), with $J = -22.2$ cm$^{-1}$, $g = 1.958$, and $C_i$ 0.0057 cm$^3$ K/mol.

paramagnetic susceptibilities of the compound. Corrected molar susceptibility data are shown in Fig. 1. A plot of inverse molar susceptibility vs temperature is shown in Fig. 2.

### *Electron Paramagnetic Resonance*

The EPR spectrum was recorded with a Bruker ER200D-SRC spectrometer operating at X-band (ca. 9.5 GHz) frequencies. The free radical DPPH ($g$ = 2.0036) was used as a field marker. The spectrum was recorded at 77 K on finely ground powder sealed in a quartz glass tube.

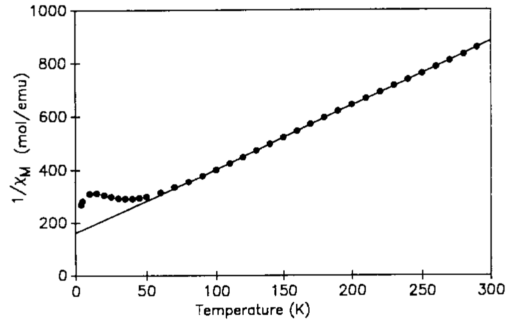

FIG. 2. Inverse molar magnetic susceptibility vs $T$ for $\beta$-LiVOPO$_4$. The solid line represents a least-squares fit to the data from 80 to 300 K according to $\chi = C/(T - \theta)$.

TABLE II

CRYSTAL DATA, INTENSITY MEASUREMENT, AND REFINEMENT PARAMETERS FOR $\beta$-LiVOPO$_4$

| | |
|---|---|
| 1. Crystal data | |
| Space group | *Pnma* (No. 62) |
| Cell constants | $a$ = 7.444(2), $b$ = 6.300 (1), $c$ = 7.174(2) Å, $V$ = 336.4(2) Å$^3$ |
| $Z$ | 4 |
| Density (calcd) | 3.334 g/cm$^3$ |
| Absorption coeff. (Mo$K\alpha$) | 32.0 cm$^{-1}$, $T_{\min, \max}$ = 0.539, 0.617 |
| 2. Intensity measurements | |
| $\lambda$ (Mo$K\alpha$) | 0.71073 Å |
| Scan mode | $\omega/2\theta$ |
| Scan rate | 2.93–14.95°/min |
| Scan width | 1.0° + $K\alpha_1$, $\alpha_2$ separation |
| Maximum $2\theta$ | 50° |
| Standard reflections | 3 every 50 reflections (no decay) |
| Reflections with $I > 2.5\ \sigma(I)$ | 307 |
| 3. Structure solution and refinement | |
| Parameters refined | 47 |
| Agreement factors[a,b] | $R$ = 0.0248, $R_w$ = 0.0278 |
| GOF | 0.760 |
| $(\Delta\rho)_{\max}$; $(\Delta\rho)_{\min}$ | 0.54 e/Å$^3$; −0.54 e/Å$^3$ |

[a] $R = \Sigma\|F_0| - |F_c\|/\Sigma|F_0|$.

[b] $R_w = [\Sigma w(|F_0| - |F_c|)^2/\Sigma w|F_0|^2]^{1/2}$, where $w = 1.0/(\sigma^2(F_0) + 0.00283\ F_0^2)$.

## Results and Discussion

### *Structure*

Table II lists the crystallographic data. Final atomic coordinates and thermal parameters are listed in Table III. Selected bond distances and angles appear in Table IV. Motif of the mutual adjunction (*22*) and bond-order sums (*23*) are given in Table V. Bond-order sums were calculated using $s = \exp[(r_0 - r)/B]$, where $B$ = 0.37 Å, $r_0$(V–O) = 1.784 Å, $r_0$(P–O) = 1.617 Å, and $r_0$(Li–O) = 1.466 Å. Bond-order sums for both the cations and anions are in good accordance with their formal oxidation states. The VO$_6$ octahedron is distorted as a result from the displacement of the V atom out of the plane through the four equatorial oxygen atoms toward one of the apical oxygen

TABLE III

ATOMIC COORDINATES AND THERMAL PARAMETERS FOR $\beta$-LiVOPO$_4$

| Atom | $x$ | $y$ | $z$ | $U_{eq}$ (Å$^2$ × 100)[a] |
|---|---|---|---|---|
| Li | ½ | 0 | 0 | 1.4(2) |
| V | 0.32631(9) | ¼ | 0.72035(9) | 0.50(3) |
| P | 0.6249(1) | ¼ | 0.3740(1) | 0.44(4) |
| O(1) | 0.4553(3) | ¼ | 0.4902(4) | 0.92(9) |
| O(2) | 0.3720(3) | −0.0556(3) | 0.7548(2) | 0.64(5) |
| O(3) | 0.2948(4) | ¼ | 0.9999(4) | 0.78(8) |
| O(4) | 0.1170(4) | ¼ | 0.6548(4) | 0.89(8) |

Anisotropic thermal parameters (Å$^2$ × 100)[b]

| | $U_{11}$ | $U_{22}$ | $U_{33}$ | $U_{23}$ | $U_{13}$ | $U_{12}$ |
|---|---|---|---|---|---|---|
| Li | 2.2(3) | 0.9(3) | 1.1(3) | 0.3(3) | −0.3(3) | −0.4(3) |
| V | 0.58(5) | 0.48(5) | 0.44(6) | 0 | 0.02(2) | 0 |
| P | 0.57(6) | 0.42(6) | 0.34(6) | 0 | −0.07(3) | 0 |
| O(1) | 0.5(2) | 1.5(2) | 0.7(1) | 0 | 0.3(1) | 0 |
| O(2) | 1.06(9) | 0.4(1) | 0.41(9) | −0.07(7) | −0.23(6) | 0.0(1) |
| O(3) | 0.4(1) | 1.1(1) | 0.8(1) | 0 | 0.1(1) | 0 |
| O(4) | 0.9(1) | 1.0(2) | 0.8(1) | 0 | −0.1(1) | 0 |

[a] Equivalent isotropic $U$ is defined as one-third of the trace of the orthogonalized $U_{ij}$ tensor.

[b] Anisotropic temperature factors are of the form: Temp = $\exp[-2\pi^2(h^2U_{11}a^{*2} + \cdots + 2hkU_{12}a^*b^* + \cdots)]$.

TABLE IV

SELECTED BOND DISTANCES (Å) AND ANGLES (°) FOR $\beta$-LiVOPO$_4$

| | | | |
|---|---|---|---|
| | Bond distances | | |
| V–O(1) | 1.910(3) | V–O(2) | 1.971(2) |
| V–O(2)*a* | 1.971(2) | V–O(3) | 2.019(3) |
| V–O(4) | 1.628(3) | V–O(4)*b* | 2.342(3) |
| P–O(1) | 1.513(3) | P–O(2)*c* | 1.534(2) |
| P–O(2)*d* | 1.534(2) | P–O(3)*e* | 1.555(3) |
| Li–O(2) | 2.031(2) | Li–O(2)*f* | 2.031(2) |
| Li–O(3) | 2.194(2) | Li–O(3)*g* | 2.194(2) |
| Li–O(4)*h* | 2.115(2) | Li–O(4)*b* | 2.115(2) |
| | Bond angles | | |
| O(1)–V–O(2) | 91.2(1) | O(1)–V–O(3) | 156.5(1) |
| O(1)–V–O(4) | 103.4(1) | O(1)–V–O(2)*a* | 91.2(1) |
| O(1)–V–O(4)*b* | 82.3(1) | O(2)–V–O(3) | 84.0(1) |
| O(2)–V–O(4) | 101.6(1) | O(2)–V–O(2)*a* | 155.4(1) |
| O(2)–V–O(4)*b* | 78.0(1) | O(3)–V–O(4) | 100.1(1) |
| O(3)–V–O(2)*a* | 84.0(1) | O(3)–V–O(4)*b* | 74.2(1) |
| O(4)–V–O(2)*a* | 101.6(1) | O(4)–V–O(4)*b* | 174.3(1) |
| O(2)*a*–V–O(4)*b* | 78.0(1) | O(1)–P–O(2)*c* | 110.1(1) |
| O(1)–P–O(2)*d* | 110.1(1) | O(1)–P–O(3)*e* | 111.0(1) |
| O(2)*c*–P–O(2)*d* | 105.9(1) | O(2)*c*–P–O(3)*e* | 109.8(1) |
| O(2)*d*–P–O(3)*e* | 109.8(1) | O(2)–Li–O(3) | 78.3(1) |
| O(2)–Li–O(2)*f* | 180.0(0) | O(2)–Li–O(3)*g* | 101.7(1) |
| O(2)–Li–O(4)*h* | 97.6(1) | O(2)–Li–O(4)*b* | 82.4(1) |
| O(3)–Li–O(2)*f* | 101.7(1) | O(3)–Li–O(3)*g* | 180.0(0) |
| O(3)–Li–O(4)*h* | 104.4(1) | O(3)–Li–O(4)*b* | 75.6(1) |
| O(2)*f*–Li–O(3)*g* | 78.3(1) | O(2)*f*–Li–O(4)*h* | 82.4(1) |
| O(2)*f*–Li–O(4)*b* | 97.6(1) | O(3)*g*–Li–O(4)*h* | 75.6(1) |
| O(3)*g*–Li–O(4)*b* | 104.4(1) | O(4)*h*–Li–O(4)*b* | 180.0(0) |

*Note*. Symmetry codes are *a*: $x, 0.5 - y, z$; *b*: $0.5 + x, y, 1.5 - z$; *c*: $1 - x, -y, 1 - z$; *d*: $1 - x, 0.5 + y, 1 - z$; *e*: $0.5 + x, y, 1.5 - z$; *f*: $1 - x, -y, 2 - z$; *g*: $1 - x, -y, 2 - z$; *h*: $0.5 - x, -y, 0.5 + z$.

atoms. This kind of deformation is characteristic of most vanadyl compounds. The distortion may be estimated by using the equation $\Delta = (\frac{1}{6})\Sigma((R_i - \bar{R})/\bar{R})^2$, where $R_i$ = an individual bond length and $\bar{R}$ = average bond length (*24*). The calculation result ($\Delta \times 10^2 = 1.11$) shows that the distortion is a little larger than those in $\alpha$-Li VOPO$_4$ ($\Delta \times 10^2 = 0.84$ for both V atoms). In $\beta$-LiVOPO$_4$ the vanadium ions are tetravalent and the octahedral distortion is much less pronounced than in $\beta$-VOPO$_4$ (*25*) ($\Delta \times 10^2 = 2.54$). The average P–O bond length in the title compound is 1.534 Å and agrees quite well with the sum of ionic radii, 1.53 Å (*24*). Interestingly, the tetrahedral distortion in $\beta$-LiVOPO$_4$ ($\Delta \times 10^5 = 9.4$) is more pronounced than that in $\beta$-VOPO$_4$ ($\Delta \times 10^5 = 2.4$). The P–O(1) bond is shortened because O(1) does not enter into the coordination sphere of the Li atom. Also consistent with this is the fact that the V–O(1) bond is shorter than other equatorial V–O bonds. The Li atom is found in a six-coordinated site with the average Li–O bond length at 2.113 Å, which is in good agreement with the sum of ionic radii (2.12 Å) (*24*). In $\alpha$-LiVOPO$_4$ the coordination numbers of the two crystallographically independent Li atoms are 5. The bond-order

TABLE V

MOTIF OF MUTUAL ADJUNCTION, COORDINATION NUMBER (C.N.), AND BOND-ORDER SUMS (Σs) IN $\beta$-LiVOPO$_4$

| | O(1) | 2 O(2) | O(3) | O(4) | C.N. | Σs |
|---|---|---|---|---|---|---|
| V | 1/1 | 2/1 | 1/1 | 2/2 | 6 | 4.19 |
| P | 1/1 | 2/1 | 1/1 | | 4 | 5.00 |
| Li | | 2/1 | 2/2 | 2/2 | 6 | 1.06 |
| C.N. | 2 | 3 | 4 | 4 | | |
| Σs | 2.03 | 2.07 | 1.99 | 2.09 | | |

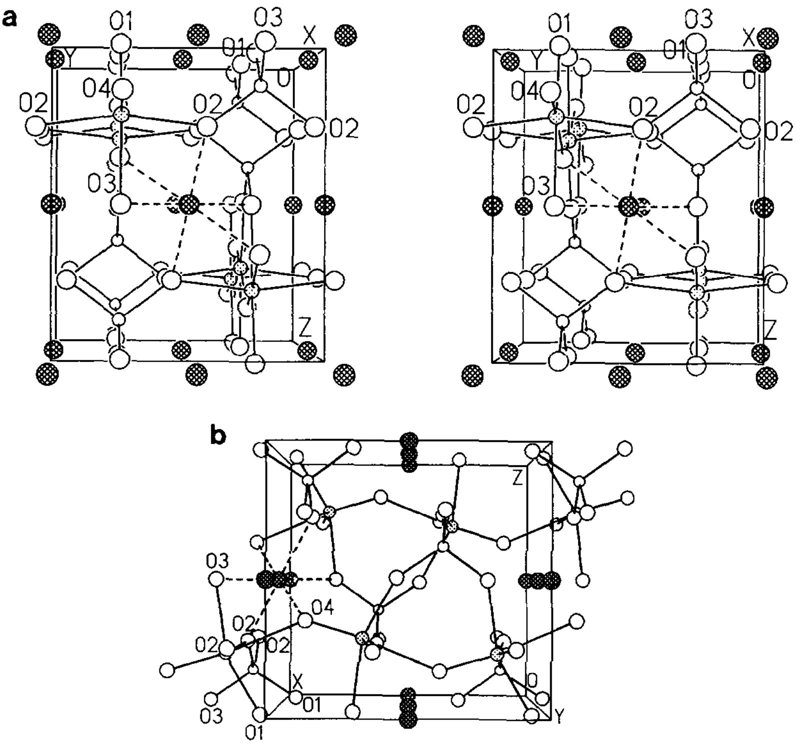

FIG. 3. (a) Stereoscopic view of the $\beta$-LiVOPO$_4$ structure along the $a$-axis. Cross-hatched circles, Li atoms; dotted circles, V atoms; small open circles, P atoms; large open circles, O atoms. (b) View of the structure along the $b$-axis.

sums for the Li atoms in the $\alpha$-polymorph are 0.89 and 0.83, suggesting that the Li atoms are loosely bound, which is also indicated by their high thermal parameters. It was predicted that the Li sites in the $\alpha$-LiVOPO$_4$ structure were able to accommodate Na atoms. We note that we have prepared NaVOPO$_4$ by high-temperature solid state reaction or by the hydrothermal method and find it structurally similar to $\alpha$-LiVOPO$_4$. The Li sites in $\beta$-LiVOPO$_4$ are smaller than those in the $\alpha$-polymorph, consistent with the higher density of the $\beta$-polymorph. A positive volume change (2.0%) accompanies the transition from $\beta$-LiVOPO$_4$ to $\alpha$-LiVOPO$_4$ since high temperature phases have more open structures and often the atoms have a lower coordination number. $\beta$-LiVOPO$_4$ was prepared at much lower temperatures than when using the normal solid state reaction method. Although this new polymorph appears thermodynamically metastable, it is kinetically stable up to about 740°C. There is close structural relationship between $\beta$-LiVOPO$_4$ and $\beta$-VOPO$_4$. The $\beta \rightarrow \alpha$-LiVOPO$_4$ transition is constructive and involves considerable bond scission and reformation between the two phases. There is no obvious structural relationship between the two polymorphs. The Madelung part of the lattice energy (MAPLE) was calculated (*26*). The MAPLE value for $\beta$-LiVOPO$_4$ is greater than that for $\alpha$-LiVOPO$_4$ by about 0.5%. MAPLE calculation does not appear useful as a guide to the relative stability of different polymorphs. Hoppe noted that MAPLE values for the different polymorphic modifications of a given composition differed only by about 1% (*26*).

As shown in Fig. 3, the structure of $\beta$-$LiVOPO_4$ consists of infinite chains of *trans*-corner-sharing $VO_6$ octahedra along the *a*-axis, which are linked together by $PO_4$ groups. The framework of the title compound is essentially the same as that of $\beta$-$VOPO_4$. These infinite chains have alternating short and long V–O bonds. Each phosphate group bonds to two adjacent octahedra in one chain, and two octahedra in two neighboring chains, introducing "kinks" into the $\cdots V{=}O\cdots V{=}O\cdots$ chains. The bond angle at the shared O atom, O(4), between two V atoms is 140.7(2)°. The chains in the title compound appear similar to those found in $\alpha$-$LiVOPO_4$. However, adjacent $VO_6$ octahedra in the chain of $\beta$-$LiVOPO_4$ have an eclipsed configuration in contrast to the staggered configuration in $\alpha$-$LiVOPO_4$. The structure of $\alpha$-$LiVOPO_4$ can be regarded as close-packed columns of vanadium oxide octahedra with each interstitial hole alternately filled with P and Li atoms. The $\beta$-polymorph also consists of close-packed columns, but every other site in each hole is filled with P atom. The Li atom in $\beta$-$LiVOPO_4$ is located between the coordination polyhedra of the V and P atoms, and is surrounded by six oxygen atoms forming a distorted octahedron with the edge lengths ranging from 2.643 to 3.404 Å. The edge lengths are much smaller than 4.24 Å, twice the sum of $Li^+$ ion and $O^{2-}$ ion radii. Consequently, the structure does not fulfill the steric condition required for fast Li ion transport.

### *Magnetic Susceptibility*

As observed in Fig. 2, the data between 80 and 300 K are described very well by a Curie–Weiss behavior: $\chi_M = C/(T - \theta)$, where $C = 0.4168$ cm$^3$ K/mol is the Curie constant and $\theta = -67.5$ K is the Weiss temperature. With increasing temperature, $\chi_M$ first decreases rapidly but reaches a minimum at $T \sim 15$ K, increases up to ~40 K, then smoothly decreases again with temperature (Fig. 1). The broad maximum at ~40 K is due to antiferromagnetic ordering of the $V^{4+}$ ions, consistent with the negative sign of the Weiss temperature. The initial decrease in $\chi_M$ with increasing temperature from 4 to 15 K is likely due to the presence of magnetic impurities. Assuming that the exchange coupling within an infinite chain is isotropic (i.e., $H = -2J\Sigma(\hat{S}_i^z\hat{S}_{i+1}^z + \hat{S}_i^x\hat{S}_{i+1}^x + \hat{S}_i^y\hat{S}_{i+1}^y)$), the magnetic susceptibility of $S = \frac{1}{2}$ ions in antiferromagnetic chains is given by Bonner and Fisher (*27*),

$$\begin{aligned}\chi_M = {} & (Ng^2\mu_B^2/kT)(0.25 + 0.14995x \\ & + 0.30094x^2) \times (1 + 1.9862x \\ & + 0.68854x^2 + 6.0626x^3)^{-1} + C_i/T, \quad (1)\end{aligned}$$

where $x = |J|/kT$ and $C_i/T$ is the Curie-like contribution from paramagnetic impurities. A quantitative fit of Eq. (1) to the whole data was obtained for reasonable values of the adjustable parameters $J = -22.2$ cm$^{-1}$, $g = 1.958$, and $C_i = 0.0057$ cm$^3$ K/mol and is shown in Fig. 1 (solid curve). The *g* value is in good agreement with that obtained from EPR study. The EPR spectrum of this compound is axially symmetric with $g_\perp = 1.968$, $g_\parallel = 1.933$, and $\langle g \rangle = (2g_\perp + g_\parallel)/3 = 1.956$. Assuming that the magnetic impurities are due to isolated $V^{4+}$ defects, the amount of the paramagnetic defects is estimated to be 1.5 mole%.

In summary, we report the hydrothermal synthesis, the structural, and magnetic properties of the metastable phase $\beta$-Li $VOPO_4$. Inexpensive quartz glass tubes are useful as reaction containers in the hydrothermal synthesis of new phases. The phase transition from the $\beta$- to the $\alpha$-polymorph is reconstructive and occurs at ~750°C. The characteristic feature of the structure of $\beta$-$LiVOPO_4$ is the infinite chains of corner-shared $VO_6$ octahedra. A good fit of the magnetic data was obtained by using the Bonner and Fisher $S = \frac{1}{2}$ linear-chain model.

## Acknowledgments

Support for this study by the National Science Council and the Institute of Chemistry Academia Sinica is gratefully acknowledged.

## References

1. K. H. Lii, Y. P. Wang, and S. L. Wang, *J. Solid State Chem.* **80,** 127 (1989).
2. K. H. Lii, H. J. Tsai, and S. L. Wang, *J. Solid State Chem.* **87,** 396 (1990).
3. K. H. Lii and S. L. Wang, *J. Solid State Chem.* **82,** 239 (1990).
4. K. H. Lii, Y. P. Wang, Y. P. Chen, and S. L. Wang, *J. Solid State Chem.* **86,** 143 (1990).
5. Y. P. Wang, K. H. Lii, and S. L. Wang, *Acta Crystallogr., Sect. C: Cryst. Struct. Commun.* **45,** 673 (1989).
6. Y. P. Wang and K. H. Lii, *Acta Crystallogr., Sect. C: Cryst. Struct. Commun.* **45,** 1210, (1989).
7. K. H. Lii and C. S. Lee, *Inorg. Chem.* **29,** 3298 (1990).
8. C. S. Lee and K. H. Lii, *J. Solid State Chem.* **92,** 362 (1991).
9. K. H. Lii and H. J. Tsai, *J. Solid State Chem.* **90,** 291 (1991).
10. K. H. Lii and H. J. Tsai, *J. Solid State Chem.* **91,** 331 (1991).
11. K. H. Lii and H. J. Tsai, *Inorg. Chem.* **30,** 446 (1991).
12. S. L. Wang, H. Y. Kang, C. Y. Cheng, and K. H. Lii, *Inorg. Chem.*, in press.
13. K. H. Lii and L. F. Mao, *J. Solid State Chem.*, in press.
14. M. L. F. Phillips, W. T. A. Harrison, T. E. Gier, G. D. Stucky, G. V. Kulkarni, and J. K. Burdett, *Inorg. Chem.* **29,** 2158 (1990).
15. A. V. Lavrov, V. P. Nikolaev, G. G. Sadikov, and M. A. Porai-Koshits, *Sov. Phys. Dokl. Engl. Transl.* **27,** 680 (1982).
16. K. H. Lii, C. H. Li, T. M. Chen, and S. L. Wang, *Z. Kristallogr.*, in press.
17. A. Rabenau, *Angew. Chem. Int. Ed. Engl.* **24,** 1026 (1985).
18. Alcock, N. W., *Acta Crystallogr., Sect. A: Found. Crystallogr.* **30,** 332 (1974).
19. G. M. Sheldrick, "SHELXTL-PLUS Crystallographic System," Version 2, Nicolet XRD Corp., Madison, WI (1987).
20. D. T. Cromer and J. T. Weber, "International Tables for X-Ray Crystallography," Vol. IV, Kynoch Press, Birmingham, England (1974).
21. P. W. Selwood, "Magnetochemistry," Interscience, New York (1956).
22. R. Hoppe, *Angew. Chem. Int. Ed. Engl.* **19,** 110 (1980).
23. I. D. Brown and D. Altermatt, *Acta Crystallogr., Sect. B: Struct. Sci.* **41,** 244 (1985).
24. R. D. Shannon, *Acta Crystallogr., Sect. A: Found. Crystallogr.* **32,** 751 (1976).
25. R. Gopal and C. Calvo, *J. Solid State Chem.* **5,** 432 (1972).
26. R. Hoppe, *in* "Crystal Structure and Chemical Bonding in Inorganic Chemistry" (C. J. M. Rooymans and A. Rabenau, Eds.), North-Holland, Amsterdam (1975).
27. J. Bonner and M. E. Fisher, *Phys. Rev. A* **135,** 640 (1964).